Neuropharmacology 84 (2014) 19–30

Contents lists available at ScienceDirect

Neuropharmacology

journal homepage: www.elsevier.com/locate/neuropharm

Transient inactivation of the ventral hippocampus in neonatal rats impairs the mesolimbic regulation of prefrontal glutamate release in adulthood

D.M. Bortz [a], C.V. Jørgensen [c], J.D. Mikkelsen [c], J.P. Bruno [a,b,*]

[a] Dept. of Psychology, The Ohio State University, Columbus, OH, USA
[b] Dept. of Neuroscience, The Ohio State University, Columbus, OH, USA
[c] Neurobiology Research Unit, University Hospital Rigshospitalet, Copenhagen, Denmark

ARTICLE INFO

Article history:
Received 16 January 2014
Received in revised form
24 March 2014
Accepted 8 April 2014

Keywords:
Schizophrenia
Animal models
Biosensor
Nucleus accumbens
TTX

ABSTRACT

Cognitive deficits in schizophrenia (SZ) reflect maturational disruptions within a neural system that includes the ventral hippocampus (VH), nucleus accumbens (NAc), basal forebrain, and prefrontal cortex (PFC). A better understanding of these changes may reveal drug targets for more efficacious cognition enhancers. We have utilized an animal model in which the above distributed system is altered, during a sensitive period of development, by transiently inactivating the VH and its efferent projections. We determined the ability of NAc shell activation to evoke prefrontal glutamate release in adult male Wistar rats that had received saline (Sal) or tetrodotoxin (TTX) as neonates (PD7) or as adolescents (PD32). The nucleus accumbens shell (NAcSh) was activated by NMDA infusions (0.05–0.30 μg/0.5 μL). Basal and evoked glutamate levels were measured amperometrically using a glutamate-sensitive microelectrode. There were no differences in basal glutamate levels among the groups tested (overall 1.41 ± 0.26 uM). However, the dose-related stimulation of prefrontal glutamate levels seen in control rats treated with saline on PD7 (4.31 ± 0.22 μM after 0.15 μg) was markedly attenuated in rats treated with TTX on PD7 (0.45 ± 0.12 μM after 0.15 μg). This effect was age-dependent as infusions of TTX on PD32 did not alter the NMDA-induced increases in glutamate release (4.10 ± 0.37 μM after 0.15 μg). Collectively, these findings reveal that transient inactivation of VH transmission, during a sensitive period of development, leads to a functional mesolimbic-cortical disconnection that produces neurochemical and ultimately cognitive impairments resembling those seen in SZ.

1. Introduction

Impairments in executive function (e.g. attention, working memory, cognitive flexibility) are considered a core symptom cluster in schizophrenia (SZ) (Thoma et al., 2007; Luck and Gold, 2008; Nuechterlein et al., 2008). Deficits in these cognitive constructs emerge prior to the initial psychotic episode (Cornblatt et al., 1999; Erlenmeyer-Kimling et al., 2000) and the severity of such impairments are predictive of long-term functional outcome in patients with SZ (Green et al., 2004; Prouteau et al., 2005). Unfortunately, they are not significantly reduced with current pharmacotherapeutics (Bowie and Harvey, 2006). Thus, there is a need to develop novel or adjunctive medications to ameliorate these cognitive symptoms through experiments on validated animal models.

There are several animal models of schizophrenic-like deficits in executive function (Lipska et al., 1995, 2002; Tseng et al., 2009; Alexander et al., 2012; Brooks et al., 2012). These models typically employ a neuronal manipulation during early development in order to mimic the neurodevelopmental anomalies believed to contribute to the disease (for review see Fatemi and Folsom, 2009). Several of these models have focused on damaging the developing hippocampus in recognition of the fact that anatomical and neurochemical dysfunctions within this structure are believed to contribute to the etiology of SZ (Harrison, 2004). One of the most widely studied animal models of SZ involves excitotoxic lesions to the ventral hippocampal region during early postnatal development (for review see (Lipska and Weinberger, 2002; Tseng et al., 2009)). Such lesions result in the gradual emergence of several cognitive deficits that parallel those seen in the schizophrenic phenotype (Mitchell et al., 2005; Tseng et al., 2008; Alexander et al.,

* Corresponding author. Department of Psychology, The Ohio State University, 1835 Neil Ave., Columbus, OH 43016, USA. Tel.: +1 614 292 1770; fax: +1 614 688 4733.
E-mail address: bruno.1@osu.edu (J.P. Bruno).

http://dx.doi.org/10.1016/j.neuropharm.2014.04.005
0028-3908/

2009; Francois et al., 2009). A limitation to this model, however, is the massive destruction of the VH. Such extensive loss of tissue is not characteristic of the patient phenotype and thus, significantly limits the face validity of the lesion model. An alternative model has recently emerged in which neuronal activity in the developing VH is transiently and reversibly inactivated using local infusions of the sodium channel blocker tetrodotoxin (TTX; (Narahashi, 1972)). Administration of TTX into the VH of rats during the first postnatal week leads to several cognitive impairments as the animals mature into young adulthood, including; latent inhibition (Meyer and Louilot, 2011), attentional set-shifting (Brooks et al., 2012), and an exaggerated locomotor response to dopamine agonists and glutamate antagonists (Lipska et al., 2002). Moreover, these animals exhibit neuronal deficits consistent with the schizophrenic pathophysiological profile, including disruptions in task-related striatal dopamine release (Meyer and Louilot, 2011) and a loss of mesolimbic regulation of cortical acetylcholine (ACh) release (Brooks et al., 2011).

Previously, we reported that N-methyl-D-aspartate (NMDA) infusions into the shell region of the nucleus accumbens produce a marked increase in prefrontal ACh levels in control rats (Zmarowski et al., 2007). In addition, local infusions of NMDA (at the same doses that stimulated prefrontal ACh release) facilitated performance on a sustained attention task when the signal detection was made more difficult by the presence of visual distractors (St Peters et al., 2011). Collectively, these data indicate that mesolimbic stimulation with NMDA may activate motivational and top-down processes that are critical as the cognitive demands of the task are elevated. We have reported that the ability of NMDA to stimulate ACh release in PFC is essentially lost in adult rats treated with TTX on PD7 but remains normal in rats treated on PD32 (Brooks et al., 2011). This loss of cholinergic transmission may contribute to observations of reduced top-down regulation in patients with SZ (for review see (Sarter et al., 2012)).

The experiments described below are designed to assess the regulation of prefrontal glutamate release in adult rats that had received intra-VH infusions of TTX or saline at various stages of development. As in our previous studies, we utilized the protocol of stimulating the Nac shell with varying concentrations of NMDA (Zmarowski et al., 2007) and measuring the effects on glutamate release in PFC using a sensitive microelectrode array with high temporal resolution (Hascup et al., 2007). The data reveal a surprisingly robust and long-lasting effect of TTX-induced inactivation of the VH; yet, the effects were highly dependent upon the age at which rats received TTX.

2. Material and methods

2.1. Subjects

Male Wistar rats (280–420 g body weight), born from breeders (Charles River Laboratories, Wilmington, MA) maintained in our breeding colony, were used as subjects in these experiments. Dams were in the colony for at least 1 mo prior to giving birth. Each litter contributed subjects for each of the four treatment conditions (see below) in order to distribute the litter variance over each condition. Upon weaning on postnatal day (PD) 21, rats were housed in groups of 2–3 until implantation of the microelectrode array (MEA) as adults (PD56-90). Animals were maintained in a temperature and humidity controlled room on a 12:12-h light:dark cycle (lights on at 06:00 a.m.) and individually housed in plastic cages lined with corn cob bedding (Harlan Teklad, Madison, WI). Animals had access to food and water ad libitum. All procedures involving animals were approved by The Ohio State University Institutional Animal Care and Use Committee in accordance with the NIH Guide for the Care and Use of Laboratory Animals. As such, all efforts were made to minimize animal suffering, to reduce the number of animals used, and to consider alternatives to *in vivo* techniques.

2.2. Drugs

Solutions used for intracranial infusion were prepared in artificial cerebral-spinal fluid (aCSF; for composition see (Brooks et al., 2011)) and adjusted to pH 7.1–7.4. n-Methyl-D-Aspartate (NMDA) and tetrodotoxin (TTX) were purchased from Sigma Aldrich Corp. (St. Louis, MO). All solutions used in preparation and calibration of the glutamate-sensitive microelectrode array (MEA) were prepared using distilled, deionized water. These include the following solutions: m-phenylenediamine dihydrochloride (mPD; Acros Organics, New Jersey, USA); L-ascorbic acid (AA), dopamine (DA), L-glutamate monosodium salt, glutaraldehyde [25% (w/w) in water], bovine serum albumin (BSA), H_2O_2, (all from Sigma Aldrich Corp., St. Louis, MO), and L-glutamate oxidase (Seikaghaku America, Inc, East Falmouth, MA).

2.3. Ventral hippocampal inactivation

2.3.1. PD7

Male neonatal rat pups received infusions of saline vehicle (PD7 Sal, $n = 6$, from 6 different litters) or tetrodotoxin (PD7 TTX, $n = 7$, from 6 different litters) into the VH at postnatal day 7 (body weight: 15–18 g). Prior to the infusions, pups were anaesthetized by hypothermia (placed on ice for 18–23 min) and then secured (head in flat position) with tape onto a Styrofoam platform that was positioned in a stereotaxic frame. An incision was made in the skin and the skull penetrated with an infusion syringe (10 μL syringe, 26G needle) at coordinates AP −3.0 mm, ML ±3.5 mm, DV −5.0 mm relative to Bregma. TTX (100 μM) was then infused into the VH in a total volume of 0.3 μL over a 3 min period. Following completion of the infusion, the needle was left in place for an additional 3 min to allow diffusion of TTX and prevent backflow up the needle tract. This infusion procedure was then repeated in the contralateral hemisphere and the scalp was closed with collodion. For saline-controls, 0.3 μL of saline (0.9%) was infused at the same rate in each hemisphere. Saline and TTX were tinted with Evans Blue (Sigma; 2.5 mg dye/1 mL saline vehicle) to identify the site of injection during histological processing of tissue after recording sessions in adults. After surgery, the pups were warmed under a lamp and returned as a group to the litter's nest area. Pups and dams were left undisturbed until weaning on PD21.

2.3.2. PD32

Male peri-adolescent rats received infusions of saline vehicle (PD32 Sal, $n = 6$, from 4 different litters) or tetrodotoxin (PD32 TTX, $n = 6$, from 5 different litters) into the VH at postnatal day 32. The general infusion procedures were identical to those used on PD7 except that rats were anesthetized with inhalant isofluorane (2%, 0.6 L/min, O_2) and TTX (100 μM, 0.3 μL) or saline (0.9%) was bilaterally infused into the VH (AP: +3.2 mm from intra-aural; L: ±4.4 mm; DV: −7.2 mm). The incision was closed with sutures and the area was swabbed with a topical antibiotic ointment (Neosporin + lidocaine). Following surgery, the animals were returned to their home cages and left undisturbed until tested as young adults (PD56).

2.4. Detection of glutamate-generated signals

Glutamate levels were detected using the microelectrode array (MEA) recording system (Quanteon, LLC, Nicholasville, KY; see Burmeister and Gerhardt, 2001). Briefly, the MEA is a ceramic microelectrode, bearing four 15 × 333 μm platinum recording sites, that interfaces with a preamplifier and the FAST-16 electrochemical recording system (See Rutherford et al., 2007 for further details on assemblage of the MEA). Each pair of recording sites on the MEA was designated to be either glutamate-sensitive (Gluox) or not (background or sentinel). The Gluox channels were coated with glutamate oxidase (2%, 1 unit/1 uL, 100 nL), BSA (1%), and glutaraldehyde (0.125%) whereas the sentinel channels were coated with just BSA and glutaraldehyde. Once the enzyme coating was allowed to cure for at least 48 h, MEAs were electro-plated with *m*-PD to block the access of larger endogenous molecules (i.e. ascorbic acid, dopamine, norepinephrine, and serotonin) to the platinum site as they would also oxidize at the applied potential (0.7 V).

The enzyme detection scheme responsible for the generation of current due to the oxidation of glutamate has been described in greater detail in previous publications (Burmeister and Gerhardt, 2001; Rutherford et al., 2007; Konradsson-Geuken et al., 2009). Briefly, glutamate is oxidized by glutamate oxidase, generating α-ketoglutarate and H_2O_2 (the reporting molecule). Because the MEA is maintained at a constant potential of +0.7 V vs. an Ag/AgCl reference electrode, the H_2O_2 is oxidized, yielding two electrons. Extracellular glutamate reaches the platinum surface of the sentinel channels, but in the absence of Gluox, any oxidation current detected reflects electroactive molecules other than glutamate. Such non-glutamate derived current is determined to be similar across each of the recording sites (see Fig. 1). The differential coating scheme allows for the isolation of current generated solely by the oxidation of glutamate by self-referencing activity of the sentinel channel from the Gluox channel (Burmeister and Gerhardt, 2001; Rutherford et al., 2007). The resulting current is then amplified and recorded.

2.5. In vitro calibration of microelectrodes

Microelectrodes were calibrated *in vitro* just prior to implantation (Hinzman et al., 2010). Calibrations were performed in a stirred solution of PBS (0.05 M, 40 ml; pH 7.4; 37 °C; +0.7 V). After a stable baseline was established, AA (250.0 μM), glutamate (3 × 20.0 μM), DA (2.0 mM), and H_2O_2 (8.8 μM), were sequentially added to the calibration beaker in 40 μL aliquots and amperometric signals were acquired at a rate of 1.0 Hz.

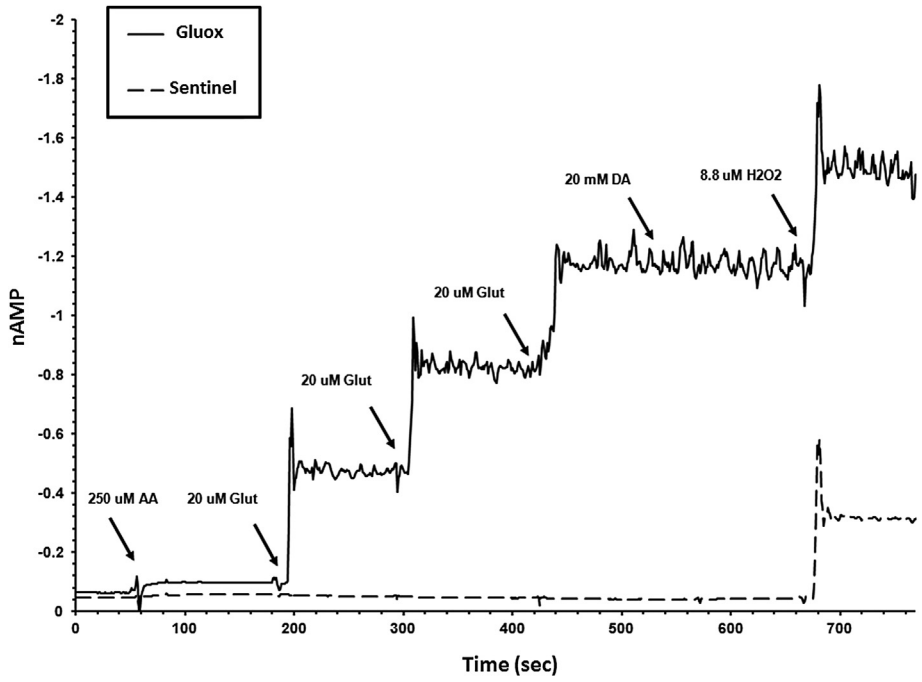

Fig. 1. A representative *in vitro* calibration of the MEA conducted immediately before implantation into the PFC. Two of the four recording channels are shown for clarity of presentation. The top tracing represents the glutamate-sensitive (Gluox) recording channel and the bottom tracing the sentinel background channel. Arrows correspond to the addition of various substances into the stirred calibration beaker. Current (nAmp) is depicted along the vertical axis and time (sec) along the horizontal axis. The successive additions of glutamate (20 μM/aliquots) produced a linear increase in current (due to the oxidation of H_2O_2 generated from glutamate) on the Gluox channel. Expectedly, there were no changes in glutamate-related current on the sentinel channel. Important for self-referencing, the calibration also reveals equivalently high sensitivities on both channels to the reporting molecule H_2O_2. The effectiveness of the *m*-PD barrier is evident by the lack of increase in current depicted following the addition of large concentrations of potential *in vivo* interferents, AA and DA, to the beaker.

Fig. 1 depicts a representative *in vitro* calibration. The tracings represent change in current detected at each of the channels following the addition (noted by the arrows) of the chemicals listed above. To simplify the figure, only two of the four channels are illustrated. The top tracing is from the glutamate sensitive channel (Gluox), whereas the bottom tracing represents the background channel (sentinel). The addition of AA produced little to no change in current on either channel. Successive additions of glutamate yielded large and consistent increases in current on only the Gluox channel. The increase in current was linear as the beaker concentration of glutamate became progressively higher. The addition of DA produced no change in current indicating the effectiveness of the *m*-PD barrier layer. Finally, the addition of H_20_2 resulted in comparable increases in current between the two channels, indicating that both recording sites are similarly sensitive to the reporting molecule. From these recordings, the sensitivity (slope, nA/μM glutamate), limit of detection (L.O.D, μM glutamate), selectivity (ratio of glutamate over ascorbic acid), and linearity (R^2) were calculated. In order to qualify for use during *in vivo* recordings, the MEAs had to conform to the following calibration criteria: (i) similar background current (i.e. no greater than a 20 pA difference) between the glutamate-sensitive and sentinel channels, (ii) linear response to increasing concentrations of glutamate ($R^2 > 0.998$), (iii) a minimum slope of −0.003 nA/μM glutamate, (iv) a minimum limit of detection of <0.5 μM, (v) a high selectivity for glutamate over either AA or DA (i.e. >50:1), and (vi) similar sensitivity to the reporting molecule H_2O_2 on all four channels (>80% similarity for each channel pair).

2.6. Implantation of microelectrodes and infusion cannulae

Animals were anesthetized with isofluorane (2%, 0.6 L/min) and implanted with the MEAs unilaterally in the PFC (in mm from bregma: AP +2.7, ML ± 0.65, DV -4.0; hemispheres counterbalanced). Stainless steel guide cannula (Plastics One, Roanoke, VA), used for intracortical infusions of NMDA, were implanted ipsilaterally in the shell of the nucleus accumbens (NAcSh; in mm from bregma: AP + 0.4, ML ± 0.70, DV − 6.4). The tip of the infusion cannula extended 1 mm beyond the end of the guide cannula. Between recording sessions, a dummy cannula, was inserted into the guide cannula and extended 0.8 mm beyond the tip of the guide. The Ag/AgCl reference electrode was implanted in the contralateral side at a site distant from the recording area. All coordinates were determined from the atlas of Paxinos and Watson (1998).

2.7. In vivo recordings and intracortical infusions

Rats receiving TTX or saline on PD7 or PD32 were tested as adults (PD56-90) in 3 recording sessions. Care was taken to test animals from each group at various points in this adult age range in order to provide comparable intervals between VH hippocampal manipulation and testing for all groups (2−3 animals from each group had a 48−54 day delay between TTX or saline injection and testing − the response of these animals was consistent with the main finding; that PD7 TTX differed from PD7 SAL or PD32 TTX). During recording sessions, rats were allowed to move freely in a wooden recording box (H 57.2 cm; W 341.9 cm; L 317.0 cm). The first day after sensor implantation consisted of placing the rats in the wooden testing box, without connecting them to the preamplifier, to allow them to habituate to their environment prior to testing. On the second day after implantation, recordings of cortical glutamate began. At the onset of each testing day, animals were placed in the recording box and connected to the preamplifier. Animals were then given approximately 3 h to establish a stable baseline before any drugs were delivered. All drugs were delivered over ~2 s (pH 7.1–7.4, 0.5 μL solutions) using a Hamilton PB600-1 manual dispenser (Hamilton Company, Reno, NV). Once the 3 h baseline period had concluded, the dummy cannula was removed and 1.0 μL of vehicle (aCSF) was delivered into the NAcSh to serve as a control infusion. Then, following a 10-min delay, one of three doses of NMDA (0.05, 0.15, 0.30 μg in 0.5 μL) was delivered into the NAcSh. Dose order was counterbalanced amongst all animals.

2.8. Histology

At the conclusion of each experiment, animals were given an overdose of Euthasol and trans-cardially perfused. Brains were removed and stored in formalin (10%) for at least 2 days, and then transferred to a sucrose solution (30%) for at least 2 days. Brains were sectioned using a cryostat; coronal sections (50 μm) were mounted on gelatin-coated slides, stained using Fast Red, and examined under a light microscope for verification of microelectrode and cannula placement. The use of the Fast Red stain also highlighted the Evan's Blue dye in the VH of the animals, thus allowing us to confirm that the TTX or saline was delivered to the correct location.

2.9. Data analysis

Measurements derived from the recording session included: (i) basal glutamate levels, (ii) maximum peak amplitude (μM) of the glutamate signal, (iii) the latency (sec) to peak onset, (iv), and duration of peak measured from peak onset to total clearance (sec). The glutamate signal, initially measured in pA, was transformed to a concentration equivalent (μM) on the basis of each sensor's individual calibration slopes generated immediately before surgery (see Fig. 1). Slopes of sentinel channels were replaced with slopes for Gluox channels to ensure equal comparison. The signal derived exclusively by the oxidation of glutamate was isolated using a self-

referencing procedure between the glutamate-sensitive recording channel and the adjacent background sentinel channel as we and others have described elsewhere (Burmeister and Gerhardt, 2001; Rutherford et al., 2007; Konradsson-Geuken et al., 2009). Comparisons were performed on all dependent measures mentioned above (basal levels, maximum peak amplitude, latency to effect, and peak duration) using analysis of variance (ANOVA) by the SPSS 18 statistics program (V19, IBM Corporations, Armonk, NY). An initial 3-way omnibus ANOVA was performed for each dependent measure using dose (0.05, 0.15, 0.30/0.5 μL) as a within-subjects factor, and age (PD7, PD32) and condition (TTX, Sal) as between-subjects factors to test for the postulated 3-way interaction. If significance was determined, post hoc 1-way ANOVAs were performed to identify the location of the significant interaction. The Huyen-Feldt correction was used to minimize the occurrence of Type II errors. A minimum number of post-hoc comparisons were conducted using independent and dependent *t-tests*. In all cases, significance was defined as $P < 0.05$.

3. Results

3.1. Verification of TTX infusion sites and MEA/cannula placements

3.1.1. TTX infusion sites

Fig. 2 provides representative photomicrographs depicting placements of TTX and saline infusions into the developing VH at PD7 (Fig. 2A and B) and PD32 (Fig. 2C and D). Injection sites were evidenced by small deposits of the Evans Blue Dye. Infusion sites appear within the VH, and any adult animals found to have infusion sites outside the VH were removed from analysis.

3.1.2. MEA and cannula placements

All subjects included in this analysis had confirmed MEA placements within the Infralimbic/Prelimbic regions of the medial PFC and infusion cannula placements within the NAcSh. Fig. 3 (left, top) contains an illustration depicting the intended placement of a PFC sensor as well as that for an infusion cannula into the NAcSh (left, bottom). As shown in the coronal photomicrographs (Fig. 3 right), the representative placements fall within their target regions (arrows indicate the ventral termination of both implantations). The PFC photomicrograph also illustrates the modest tissue damage produced by the MEA compared to conventional microdialysis probes.

3.2. Mesolimbic regulation of glutamate release in PFC depends upon age at the time of hippocampal inactivation

In order to determine whether transient inactivation of the VH of neonatal rats was sufficient to disrupt NMDA-mediated increases in PFC glutamate levels, NMDA was administered into the NAcSh of adult rats treated with saline or TTX on either PD7 or PD32. NMDA was injected into NAcSh in three counterbalanced doses (0.05, 0.15, and 0.30 μg in 0.5 μL). Fig. 4 displays representative tracings of the MEA's electrochemical signal generated in adults, treated with saline vehicle (top) or TTX (bottom) on PD7, following the low dose of NMDA (0.05 μg). In this figure, the top tracing represents the signal generated by the glutamate-sensitive channel (Gluox), and the middle tracing represents the signal generated from the sentinel channel. The sentinel channels are sensitive to everything that the Gluox channels are except for glutamate. The bottom tracing represents the resulting signal generated from subtracting the background channel from the glutamate-sensitive channel. Thus, this bottom tracing and all subsequent tracings indicate the self-referenced signal, which is the signal generated exclusively by the oxidation of glutamate. Inspection of the self-referenced glutamate tracings from both groups reveals the stability of each baseline both before and after the drug effect. Basal values of glutamate did not differ between saline (1.40 ± 0.51 μM) and TTX-treated rats (1.83 ± 0.55 μM; $P > 0.5$). Intra-NAcSh infusions of NMDA into the saline-controls (top) resulted in a delayed (~40 s) increase in extracellular levels that rapidly reached maximum amplitude (glutamate concentration; 2.19 μM) and was cleared to baseline in 10 s. The clearance timing of these evoked glutamate responses has been seen previously (Bortz et al., 2013). The NMDA-induced increases in glutamate signal were not the result of the infusion

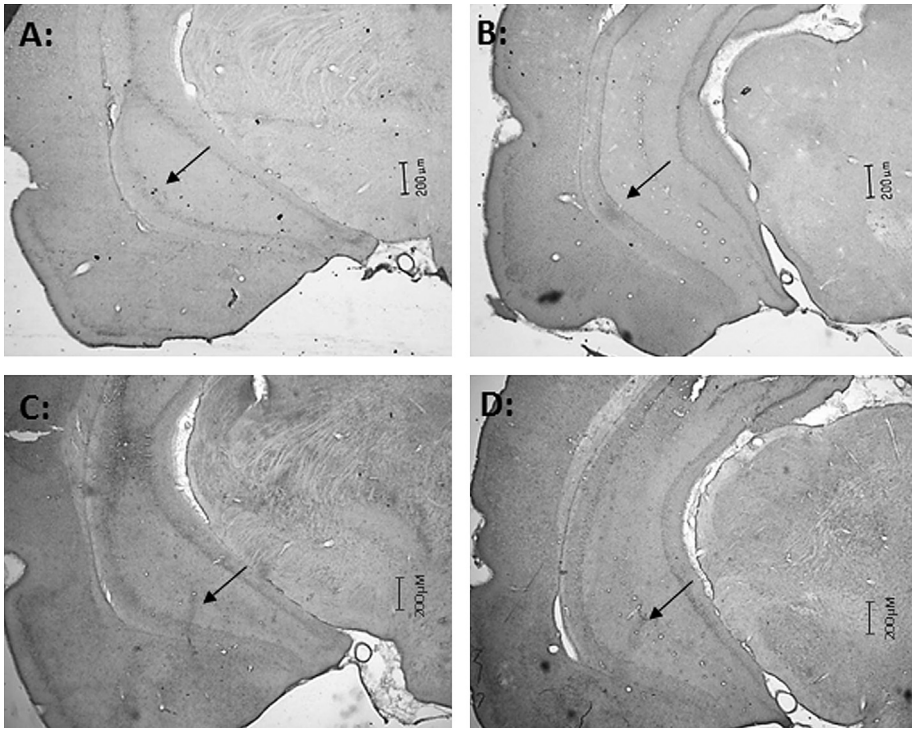

Fig. 2. Photomicrograph depicting representative sites of infusion for TTX and saline in adult rats treated with saline or TTX on PD7 (1A, 1B respectively) or on PD32 (2A, 2B, respectively). Each placement was in the VH. Placements that fell outside of the VH were not included in the analysis.

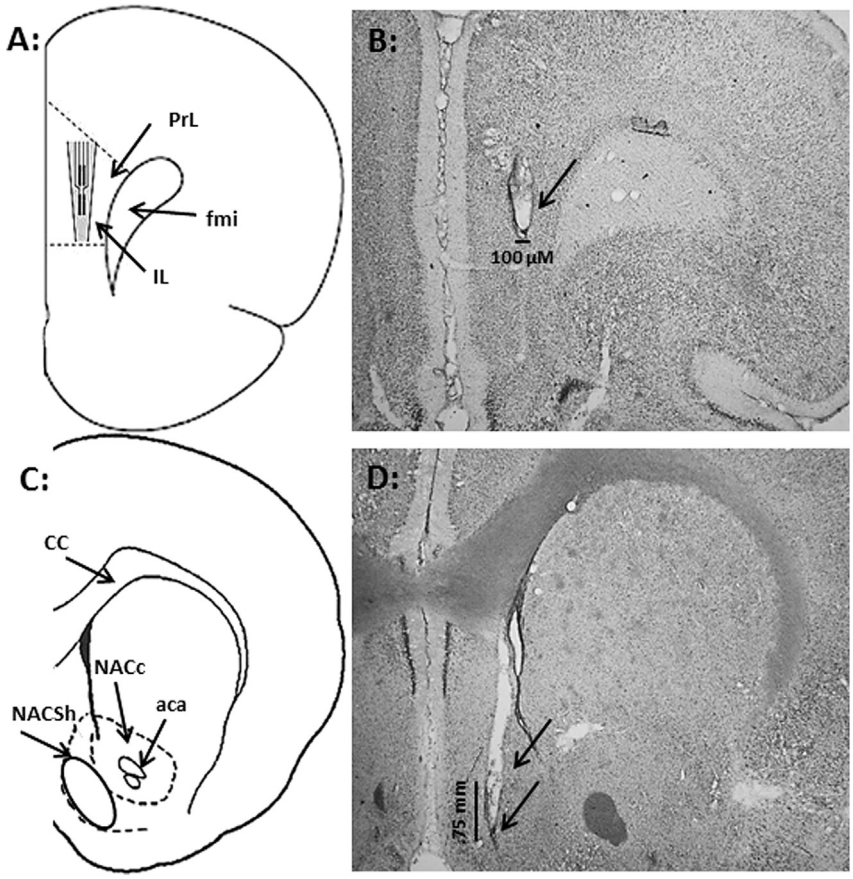

Fig. 3. An illustration depicting the intended placement of an MEA sensor in PFC (left top) as well as that for an infusion cannula into the NAcSh (left, bottom). As shown in the representative coronal photomicrographs (Fig. 3 right), implantations were located within their target regions (arrows indicate the ventral termination of both placements).

process *per se* as artificial CSF vehicle infusions, conducted prior to drug delivery, did not result in any significant change from baseline. The self-referenced tracings from NMDA infusions into TTX-treated rats (bottom) reveal a markedly attenuated glutamate release (glutamate increase did not reach 3× noise criteria; designated = 0.0 μM;), relative to the effects of NMDA in saline-treated controls.

Fig. 5 displays representative tracings of the *self-referenced* signal generated in adult rats, treated with saline (top) and TTX (bottom) on PD7, after having received the middle and high doses of NMDA (0.15 and 0.30 μg). Inspection of the self-referenced glutamate tracings from saline controls (top) reveal that intra-NAcSh infusions of NMDA resulted in a delayed (35–50 s) increase in extracellular levels that rapidly reached maximum amplitude (4.69 and 5.22 μM) and was cleared to baseline in 20–40 s. The self-referenced tracings from NMDA infusions into TTX-treated rats (bottom) reveal a markedly attenuated glutamate release (0.0 and 0.56 μM), relative to the effects of NMDA in saline-treated controls.

Representative records of the MEA's electrochemical signal generated in adults, treated with saline vehicle or TTX on PD32, following the low dose of NMDA (0.05 μg) are illustrated in Fig. 6. In this figure, the top tracing represents the signal generated by the glutamate-sensitive channel (Gluox), and the middle tracing represents the signal generated from the sentinel channel. The bottom tracing indicates the signal generated exclusively by the oxidation of glutamate. Inspection of the self-referenced glutamate tracings from both groups reveals the stability of each baseline both before and after the NMDA effect. Basal values of glutamate did not differ between saline (1.49 ± 0.55 μM) and TTX-treated rats (0.65 ± 0.20 μM; $P > 0.1$). Intra-NAcSh infusions of NMDA into the saline-controls (top) resulted in a delayed (~40 s) increase in extracellular levels that rapidly reached maximum amplitude (glutamate concentration; 2.60 μM) and was cleared to baseline in ~20 s. The NMDA-induced increases in glutamate signal were not the result of the infusion process *per se* as artificial CSF vehicle infusions, conducted prior to drug delivery, did not result in any significant change from baseline.

In marked contrast to the effects seen in rats treated with TTX on PD7, the self-referenced tracings from NMDA infusions into rats treated with TTX on PD32 (bottom) reveal an NMDA evoked increase in glutamate levels that were similar in amplitude (3.13 μM) and duration (~20 s) to that seen in control rats receiving saline on PD7.

Fig. 7 displays representative tracings of the *self-referenced* signal generated in adult rats, treated with saline and TTX on PD32, after having received the intermediate and high doses of NMDA (0.15 and 0.30 μg). Inspection of the self-referenced glutamate tracings from saline controls (top) reveal that intra-NAcSh infusions of NMDA resulted in a delayed (35–50 s) increase in extracellular levels that rapidly reached maximum amplitude (glutamate concentration; 4.37 and 4.25 μM) and was cleared to baseline in 20–40 s. As with the low dose of NMDA, the intermediate and high doses of NMDA (0.15 and 0.30 μg) given to the PD32 TTX rats resulted in large (4.35 and 7.87 μM) and transient (20–40 s) PFC glutamate increases, similar to those seen in the PD32 saline rats.

In terms of the group data (Fig. 8), basal glutamate levels did not differ significantly between the two inactivation conditions; the two ages, nor across the doses of NMDA (All *P*'s > 0.05). An overall

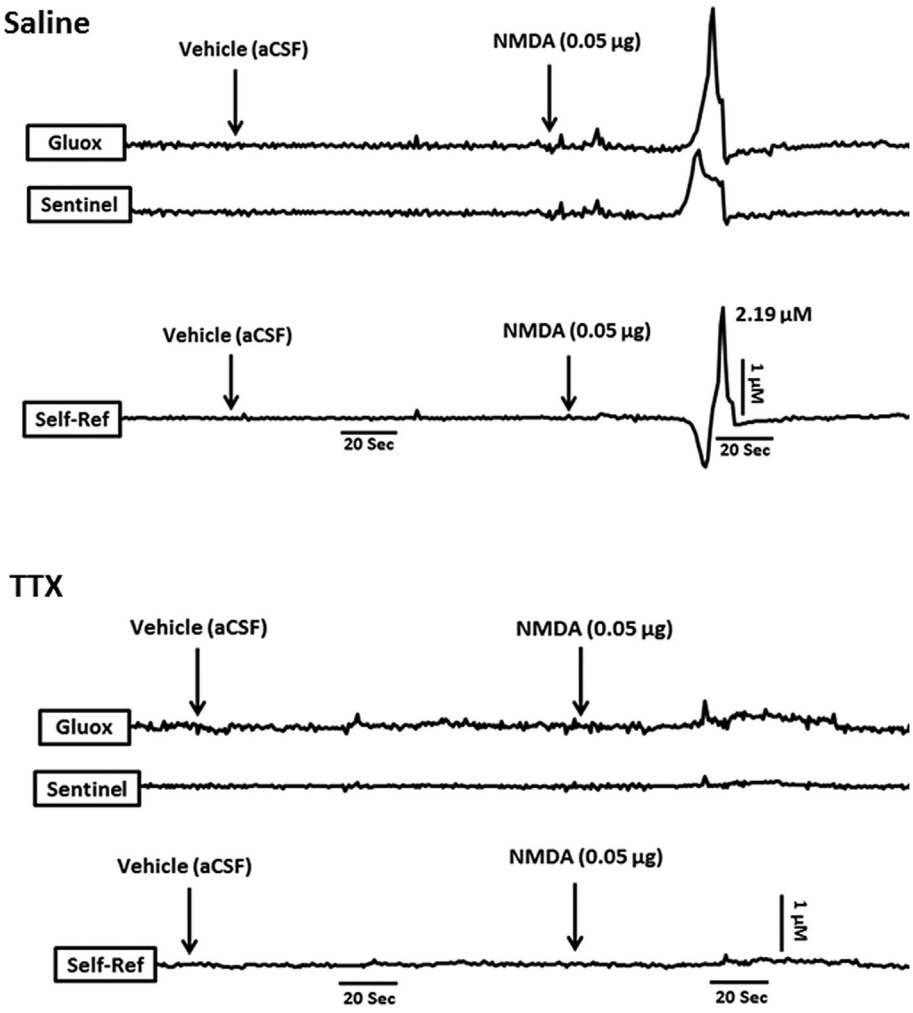

Fig. 4. Representative MEA recordings from the PFC of adult rats treated with intra-VH saline (top) or intra-VH TTX (bottom) on PD7. In these sessions, rats received both an intra-NAc infusion of vehicle (aCSF) and the low dose of NMDA (0.05 µg). The top tracing represents the signal from the glutamate-sensitive channel (Gluox), whereas the middle tracing represents the signal from its adjacent sentinel or background channel. The bottom tracing (Self Ref) represents the signal derived from subtracting the second channel from the first, thereby isolating the signal obtained exclusively from the oxidation of extracellular glutamate. Changes in the vertical axis are transformed (using the regression lines from the calibration) from current to concentration (µM), whereas the horizontal axis reflects the passage of time (sec). Arrows represent the time at which infusions were delivered. Focusing on the self-referenced tracings, the local infusion of the aCSF vehicle did not produce a significant change from baseline in either condition. In the rat treated with saline on PD7, intra-NAcSh infusions of NMDA (0.05 µg) produced a robust (2.19 µM, from baseline) increase in prefrontal glutamate release, that persisted for ~12 s before returning to a stable baseline. In contrast, in the rat treated with TTX on PD7, the NMDA infusion failed to stimulate glutamate levels beyond those seen at baseline.

ANOVA revealed highly significant effects of NMDA dose ($F_{2,42} = 47.42$, $P < 0.001$), inactivation condition ($F_{1,21} = 37.71$, $P < 0.001$), age ($F_{1,21} = 56.06$, $P < 0.001$) and, importantly, a dose × condition × age interaction ($F_{2,42} = 15.31$, $P < 0.001$). Subsequent analyses revealed the sources of this interaction to be 1) an almost complete loss of NMDA-evoked glutamate release when animals were treated with TTX as neonates (PD7) and 2) the preservation of control-like, dose-dependent NMDA-evoked glutamate release when animals were treated with TTX as adolescents (PD32).

Finally, there were no significant effects of age, inactivation condition, or dose on the clearance of evoked glutamate back to basal values (all *P's* > 0.05). The mean (±S.E.M.) T_{80} values for PD7 Sal, PD7 TTX, PD32 Sal, and PD32 TTX were 17.24 ± 3.77, 14.91 ± 4.62, 10.71 ± 1.43, and 10.13 ± 1.69, respectively.

4. Discussion

The results of these experiments indicate that activation of the shell region of the NAc with NMDA dose-dependently increases extracellular glutamate levels in the medial prefrontal cortex in saline-treated control rats. Transient inactivation of the developing VH results in nearly a complete loss of this mesolimbic regulation of prefrontal glutamate levels. This effect displays a clear sensitive period as TTX administration during the neonatal period (i.e. PD7) yields dysregulation of cortical glutamatergic transmission whereas inactivation during early adolescence (i.e. PD32) does not. The discussion that follows focuses on several issues related to these findings, including; a) evidence that the self-referenced electrochemical signal is indeed glutamate; b) the modulation of prefrontal glutamate levels by accummbal NMDA receptors; c) the potential age-dependent consequences of transient inactivation of the VH; and d) implications of this model for research on the cognitive deficits associated with SZ.

4.1. Evidence that the self referenced electrochemical signal is glutamate

The results from several studies collectively support the interpretation that the self-referenced electrochemical signals from the

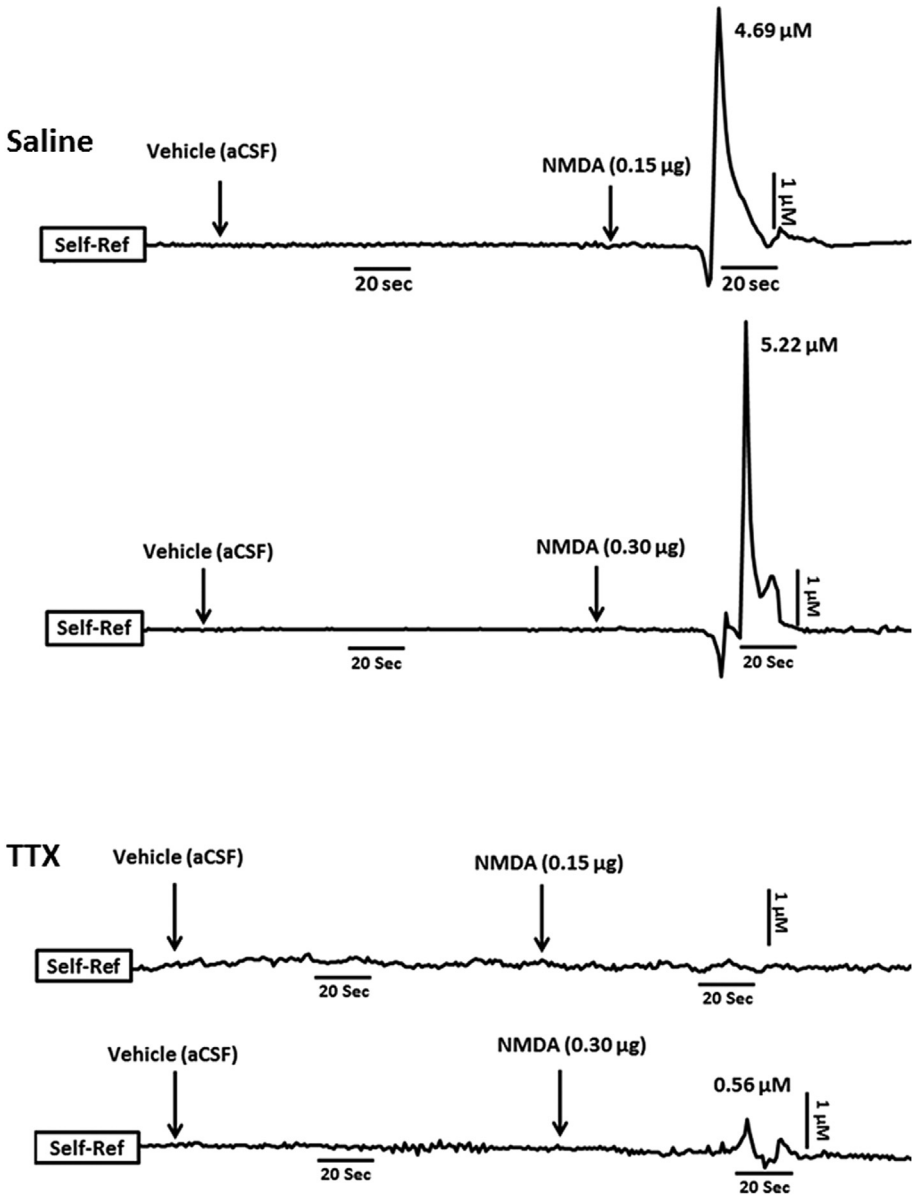

Fig. 5. Two representative MEA self-referenced recordings from the PFC of adult rats treated with intra-VH saline (top) or intra-VH TTX (bottom) on PD7. In these sessions, on consecutive days, rats received an intra-NAcSh infusion of vehicle (aCSF) and either the intermediate dose (0.15 µg) or highest dose (0.30 µg) of NMDA in counterbalanced order. As in Fig. 4, intra-NAcSh infusions of vehicle (aCSF) were without effect. In the rat treated with saline, NMDA infusions led to dose-related increases in glutamate release (4.69 and 5.22 µM, from baseline) that reached maximum levels within 1sec and were cleared to baseline in ~20 s. However, in the rat treated with TTX, the NMDA-evoked glutamate release was markedly attenuated; still without response following 0.15 µg and with an ~90% reduction following 0.30 µg.

MEA represent the current generated exclusively by the oxidation of glutamate at the surface of the electrode. First, administration of ceftriaxone or TβOA, drugs that enhance (Wei et al., 2012) or suppress (Shimamoto et al., 1998) excitatory amino acid transporters respectively, bi-directionally affect the amplitude and/or clearance of the self-referenced glutamate peak (Bortz et al., 2013). Second, the local infusion of extracellular glutamate standards yields differences between the Gluox and sentinel sites that resemble those seen here. Finally, recordings at +0.25 V, a value lower than the oxidation potential of the glutamate recording molecule H_2O_2, yet larger than many potential endogenous interferents, generate wave forms that are equivalent on both the Gluox and sentinel sites (i.e. no detectable glutamate; unpublished observations).

Two major glutamatergic afferents to PFC are from the mediodorsal thalamus (Leonard, 1969; Guldin et al., 1981; Groenewegen, 1988; Hoover and Vertes, 2007) and the ventral hippocampus (Ferino et al., 1987; Jay and Witter, 1991; Jay et al., 1992; Hoover and Vertes, 2007). Release from both inputs is modulated by presynaptic nicotinic ACh receptors (Gray et al., 1996; Gioanni et al., 1999; Lambe et al., 2003). The contribution of each of these inputs to the extracellular glutamate being measured in the present experiments remains to be determined. We are currently studying the impact of selective lesions of these input regions on basal and evoked glutamate levels.

4.2. Mesolimbic regulation of cortical glutamate levels

In this and other papers, we have used intra-NAcSh perfusions (200–400 uM) or infusions (0.05–0.30 µg/0.5 µL) of NMDA. The selection of this manipulation to stimulate prefrontal glutamate release was based upon two important observations previously reported by our group. First, intra-NAcSh perfusions or infusions of

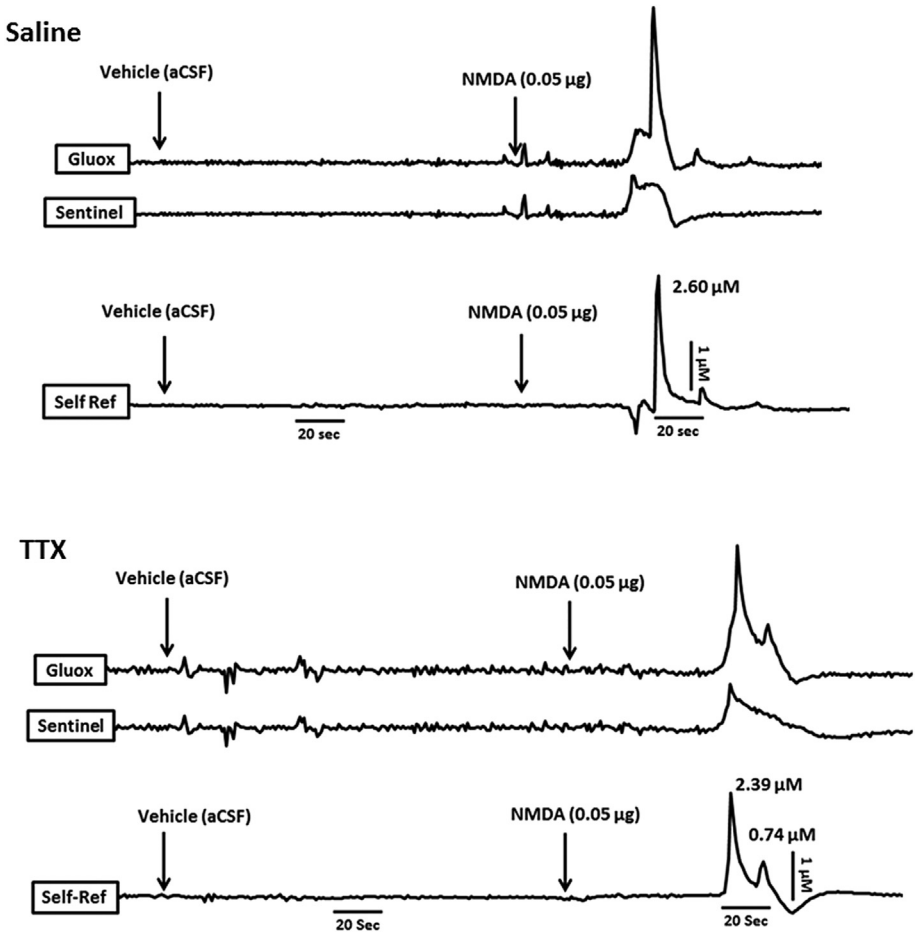

Fig. 6. Representative MEA recordings from the PFC of adult rats treated with intra-VH saline (top) or intra-VH TTX (bottom) on PD32. In these sessions, rats received both an intra-NAc infusion of vehicle (aCSF) and the low dose of NMDA (0.05 µg). As in Fig. 4, the top tracing represents the signal from the glutamate-sensitive channel (Gluox) and the middle tracing represents the signal from its adjacent sentinel or background channel. The bottom tracing (Self Ref) isolates the signal obtained exclusively from the oxidation of extracellular glutamate. Focusing on the self-referenced tracings, the local infusion of the aCSF vehicle continued not to produce a significant change from baseline in either condition. In the rat treated with saline on PD32, intra-NAcSh infusions of NMDA (0.05 µg) produced a significant (2.60 µM, from baseline) increase in prefrontal glutamate release, that persisted for ~20 s before returning to a stable baseline. In contrast to the rat that received TTX on PD7 (Fig. 4), the rat treated with TTX on PD32 exhibited a control-like response to NMDA infusion (3.13 µM from baseline; represents the sum of the two evoked glutamate peaks).

these doses of NMDA stimulate the release of ACh in PFC (Neigh et al., 2004; Zmarowski et al., 2007) thereby providing an endogenous substrate (ACh and/or choline) to stimulate cortical α7 nicotinic ACh receptors (relevant to mechanism proposed below). Second, we have reported that intra-NAcSh infusions of NMDA restore performance in a sustained attention task that was disrupted by the addition of visual distractors (St Peters et al., 2011). Thus, the intra-NAcSh NMDA stimulus (and the doses that we employed) are linked to clear, positive, performance outcomes in tests of a cognitive construct (cue detection, sustained attention) that is impaired in schizophrenics (Pantelis et al., 1997; Cattapan-Ludewig et al., 2005; Hilti et al., 2010).

The circuitry specifically linking the activation of NAcSh NMDA receptors to an increase in prefrontal extracellular glutamate levels remains to be determined. Previously, we demonstrated that cortical cholinergic inputs from basal forebrain were necessary for the intra-NAcSh NMDA-mediated increases in prefrontal ACh levels and the reinstatement of task performance (St Peters et al., 2011). As we propose that stimulation of local nicotinic ACh receptors is contributing to the evoked glutamate levels, we are currently testing the hypothesis that the NMDA infusions lead to an activation of the basal forebrain cortical cholinergic system and the resultant local increase in α7 nicotinic ACh receptor activity stimulates glutamate release from afferents originating in the medial dorsal thalamus and or VH.

4.3. Age-dependency of VH transient inactivation

Several studies have revealed the significant impact of insults to the perinatal VH on neuroanatomical and cognitive effects that are similar to those discussed with respect to SZ. This is not surprising given the prominent role that developmental anomalies within hippocampus are thought to play a role in the etiology of SZ (For review, see (Harrison, 2004)). For two decades, the most popular animal model of SZ involved excitotoxic lesions of the VH during the first postnatal week of development (For review, see Tseng et al., 2009). In terms of the current paper, we reported that permanent damage to the developing VH block the ability of intra-NAcSh NMDA infusions to evoke ACh levels in PFC (Alexander et al., 2009). Importantly, rats sustaining similar lesions at PD32 still exhibited the control-like increase in prefrontal ACh levels. Given the realization that the hippocampal pathophysiology in SZ was more restricted than the large gaping loss of tissue involved in the lesion animal models, several investigators began using a non-lesion approach by transiently inactivating neuronal activity in the VH (Lipska et al., 2002; Meyer and Louilot, 2011; Brooks et al.,

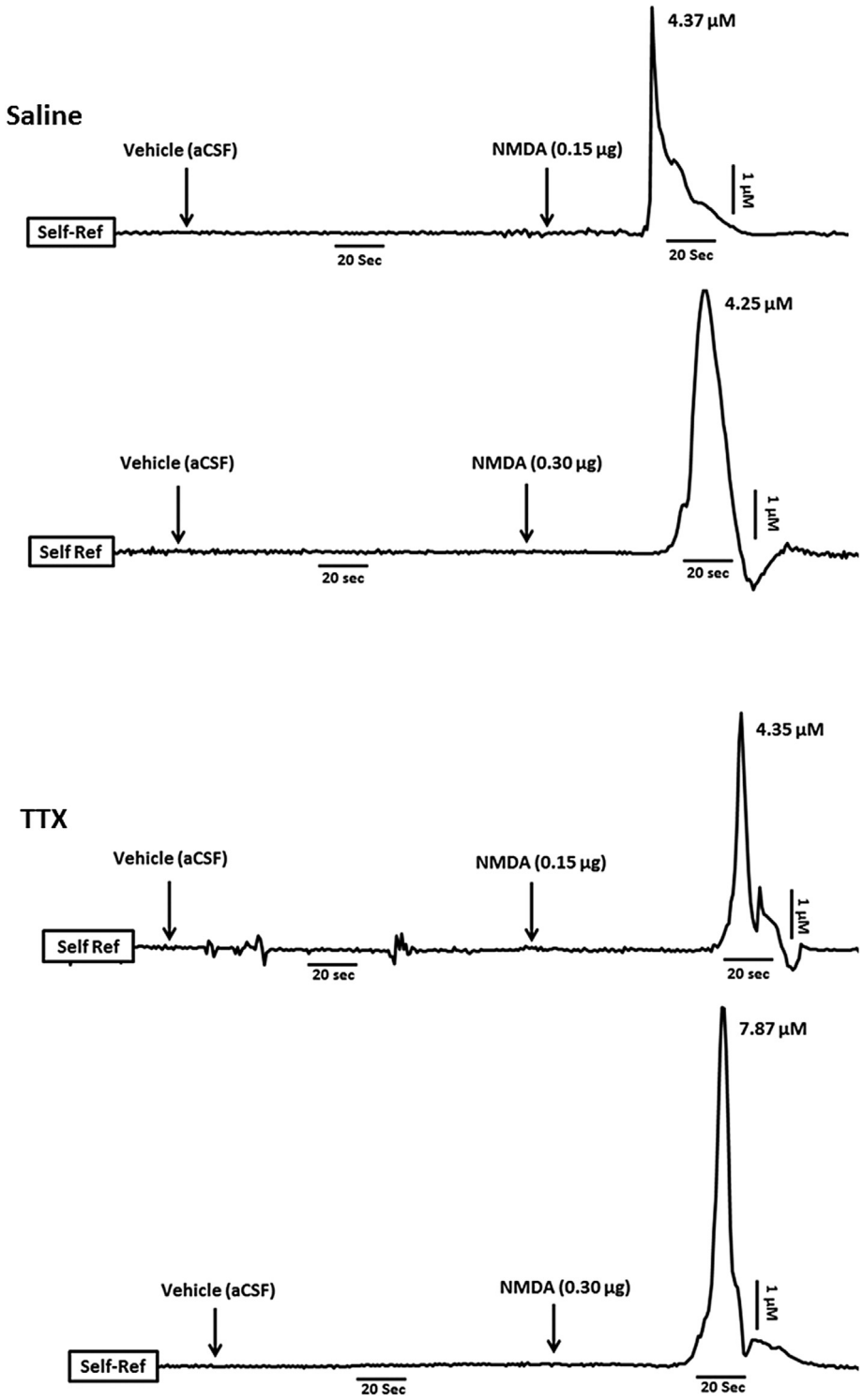

Fig. 7. Two representative MEA self-referenced recordings from the PFC of adult rats treated with intra-VH saline (top) or intra-VH TTX (bottom) on PD32. In these sessions, on consecutive days, rats received an intra-NAcSh infusion of vehicle (aCSF) and either the intermediate dose (0.15 µg) or highest dose (0.30 µg) of NMDA in counterbalanced order. As in previous figures, intra-NAcSh infusions of vehicle (aCSF) were without effect. In the rat treated with saline, NMDA infusions led to comparable increases in glutamate release after both doses (4.37 and 4.25 µM, from baseline) that reached maximum levels within 1sec and were cleared to baseline in ~25 s. Unlike the case in the rat treated with TTX on PD32 (Fig. 5), the rat treated with TTX as an adolescent exhibited a control-like NMDA-evoked glutamate release (4.35 and 7.87 µM, from baseline).

2012). The transient inactivation during a sensitive period of development presumably affected the maturation of VH as well as its principal targets, the PFC and NAc (Brooks et al., 2011; Meyer and Louilot, 2011). Interestingly, the effects of transient inactivation paralleled those seen following permanent excitotoxic lesions. Thus, TTX infusions on PD7, but not on PD32, markedly attenuated the increase in prefrontal ACh levels seen in control rats (Brooks et al., 2011).

It should be noted that in our studies PD7 and PD32 rats differ in terms of the duration between the infusion of TTX and the testing

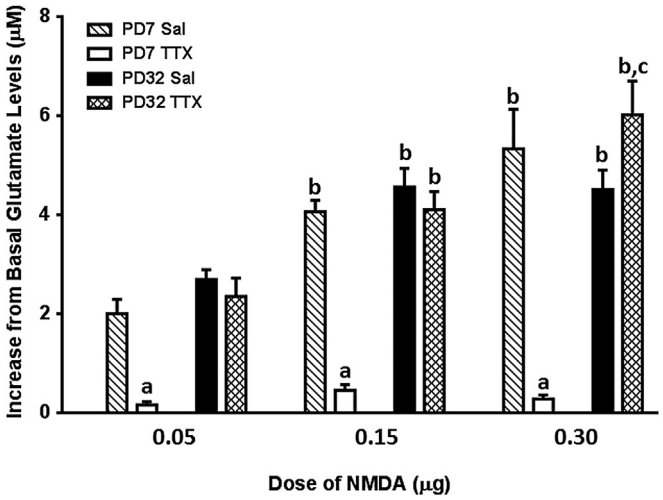

Fig. 8. Group data of evoked prefrontal glutamate release (mean ± S.E.M.) as a function of NMDA dose infused into the shell region of the NAc. The dose of NMDA is a within-subject, counterbalanced factor. This figure highlights the highly significant interaction among age, inactivation condition, and dose of NMDA. The control groups, PD7 Sal ($n = 6$) and PD32 Sal ($n = 6$) as well as rats treated with TTX on PD32 ($n = 6$) exhibited a similar dose related response to NMDA in which the intermediate and highest doses evoked greater glutamate increases from baseline than the response following the lowest dose ($^{b} = P < 0.00$). In fact, the PD32 TTX group following the 0.30 dose exhibited a greater response to NMDA than the PD32 TTX group following the 0.05 dose ($^{c} = P < 0.01$). The lack of responsivity in the PD7 TTX group ($n = 7$), to any dose of NMDA, stands in marked contrast to any of the other 3 groups ($^{a} = P < 0.001$).

for evoked glutamate release. PD7 rats were tested 49–78 days after infusions. PD32 rats were tested 24–48 days after infusions. However, there were 2–3 rats from each of the 4 treatment conditions tested 48–54 days after the SAL or TTX infusions; yet these animals still revealed the marked difference between PD7 TTX and PD32 TTX. Thus, we do not believe the post TTX interval to be a main factor in determining these age-dependent effects. The two age groups also differed in terms of the anesthesia utilized (PD7/hypothermia vs PD32/isoflurane). This was necessary as we experienced a high degree of mortality with isoflurane in the younger pups. Thus, it is conceivable that the age-dependent effects were influenced by an interaction between TTX and the anesthetic. We discounted this possibility for 2 reasons; 1) one would need to presume that TTX did not exhibit its expected blockade of sodium channels in the presence of isoflurane (as PD32 TTX were identical to PD32 SAL) yet several electrophysiological studies have measured this effect in rats anesthetized with isoflurane (Zhang et al., 2010; Westphalen et al., 2011) and 2) we observed similar age-related differences between the effects of TTX at PD7 and PD32 on evoked ACh levels in PFC (Brooks et al., 2012) as we report here with evoked glutamate in PFC.

This age-dependency suggests that neurodevelopmental events critical to the functional maturation of the PFC, NAc, and BF distributed system are ongoing during the first postnatal week, but are more mature and stable, at least for the regulation of cortical ACh and glutamate, later in development. At least two mechanisms could account for these early developmental effects on chemotransmission. First, TTX infusions on PD7 may produce functional deficits in the subsequent development of local GABAergic interneurons that regulate the maturation of the above mentioned VH efferents to PFC and NAc (Lipska et al., 2003; Francois et al., 2009). TTX infusions at later ages may fall outside of a critical window for target maturation as these inputs are establishing synaptic contacts in cortex from PD11 to PD20 (Sutor and Luhmann, 1995). Second, the anomalous maturation of these contacts and subsequent information flow may lead to reduced spine density in frontal cortex. In cultured granule cells, the formation of mature dendritic spines was reduced following exposure to TTX (Drakew et al., 1999). These results are consistent with a reduction in cortical and hippocampal spine density in the brains of patients with SZ (Lewis and Gonzalez-Burgos, 2008).

4.4. Implications for the cognitive deficits seen in schizophrenia

Several studies have demonstrated cognitive deficits following early transient inactivation of the VH and many of these impairments are functionally related to those seen in SZ. For example, in a series of studies using infusions of TTX into VH at PD7, Louilot and colleagues have reported deficits in performance in a latent inhibition task (Meyer and Louilot, 2011). These deficits correlated with abnormalities in dopaminergic transmission within the NAc (Peterschmitt et al., 2008; Meyer et al., 2009). We have reported that adult rats, sustaining early transient inactivation on PD7, but not on PD32, exhibit impaired performance during the reversal and extra-dimensional shift stages of a task of cognitive flexibility (Brooks et al., 2012). Given the critical role of prefrontal glutamatergic (Stefani and Moghaddam, 2005), and cholinergic transmission (Brooks et al., 2011, 2012) for cognitive flexibility, the present deficits in the mesolimbic regulation of prefrontal glutamate release may contribute to these cognitive impairments.

Collectively, these studies suggest that transient inactivation of the perinatal VH represents a valid animal model for studying neurochemical and cognitive impairments seen in SZ. As such, the animal model may present a valuable platform for the rational testing of cognition-enhancing drugs for the treatment of deficits in executive function.

Acknowledgments

This research was supported by a grant from the Danish Council for Strategic Research (COGNITO), the NOVO Nordisk Foundation, and the Lundbeck Foundation.

Abbreviations

AA	ascorbic acid
ACh	acetylcholine
aCSF	artificial cerebrospinal fluid
ANOVA	analysis of variance
BSA	bovine serum albumin
DA	dopamine
Gluox	glutamate sensitive
MEA	microelectrode array
NAc	nucleus accumbens
NAcSh	nucleus accumbens shell
NMDA	N-methyl-D-aspartate
PD	post-natal day
PFC	prefrontal cortex
PD7 TTX	animals treated with tetrodotoxin as neonates
PD7 Sal	animals treated with saline as neonates
PD32 TTX	animals treated with tetrodotoxin as adolescents
PD32 Sal	animals treated with saline as adolescents
SZ	schizophrenia
TTX	tetrodotoxin
VH	ventral hippocampus

References

Alexander, K.S., Brooks, J.M., Sarter, M., Bruno, J.P., 2009. Disruption of mesolimbic regulation of prefrontal cholinergic transmission in an animal model of

schizophrenia and normalization by chronic clozapine treatment. Neuropsychopharmacology 34, 2710–2720.
Alexander, K.S., Wu, H.Q., Schwarcz, R., Bruno, J.P., 2012. Acute elevations of brain kynurenic acid impair cognitive flexibility: normalization by the alpha7 positive modulator galantamine. Psychopharmacol. Berl. 220, 627–637.
Bortz, D.M., Mikkelsen, J.D., Bruno, J.P., 2013. Localized infusions of the partial alpha 7 nicotinic receptor agonist SSR180711 evoke rapid and transient increases in prefrontal glutamate release. Neuroscience 255, 55–67.
Bowie, C.R., Harvey, P.D., 2006. Cognitive deficits and functional outcome in schizophrenia. Neuropsychiatr. Dis. Treat. 2, 531–536.
Brooks, J.M., Pershing, M.L., Thomsen, M.S., Mikkelsen, J.D., Sarter, M., Bruno, J.P., 2012. Transient inactivation of the neonatal ventral hippocampus impairs attentional set-shifting behavior: reversal with an alpha7 nicotinic agonist. Neuropsychopharmacology 37, 2476–2486.
Brooks, J.M., Sarter, M., Bruno, J.P., 2011. Transient inactivation of the neonatal ventral hippocampus permanently disrupts the mesolimbic regulation of prefrontal cholinergic transmission: implications for schizophrenia. Neuropsychopharmacology 36, 2477–2487.
Burmeister, J.J., Gerhardt, G.A., 2001. Self-referencing ceramic-based multisite microelectrodes for the detection and elimination of interferences from the measurement of L-glutamate and other analytes. Anal. Chem. 73, 1037–1042.
Cattapan-Ludewig, K., Hilti, C.C., Ludewig, S., Vollenweider, F.X., Feldon, J., 2005. Rapid visual information processing in schizophrenic patients: the impact of cognitive load and duration of stimulus presentation. A pilot study. Neuropsychobiology 52, 130–134.
Cornblatt, B., Obuchowski, M., Roberts, S., Pollack, S., Erlenmeyer-Kimling, L., 1999. Cognitive and behavioral precursors of schizophrenia. Dev. Psychopathol. 11, 487–508.
Drakew, A., Frotscher, M., Heimrich, B., 1999. Blockade of neuronal activity alters spine maturation of dentate granule cells but not their dendritic arborization. Neuroscience 94, 767–774.
Erlenmeyer-Kimling, L., Rock, D., Roberts, S.A., Janal, M., Kestenbaum, C., Cornblatt, B., Adamo, U.H., Gottesman II, , 2000. Attention, memory, and motor skills as childhood predictors of schizophrenia-related psychoses: the New York high-risk project. Am. J. Psychiatry 157, 1416–1422.
Fatemi, S.H., Folsom, T.D., 2009. The neurodevelopmental hypothesis of schizophrenia, revisited. Schizophr. Bull. 35, 528–548.
Ferino, F., Thierry, A.M., Glowinski, J., 1987. Anatomical and electrophysiological evidence for a direct projection from Ammon's horn to the medial prefrontal cortex in the rat. Exp. Brain Res. 65, 421–426.
Francois, J., Ferrandon, A., Koning, E., Angst, M.J., Sandner, G., Nehlig, A., 2009. Selective reorganization of GABAergic transmission in neonatal ventral hippocampal-lesioned rats. Int. J. Neuropsychopharmacol. 12, 1097–1110.
Gioanni, Y., Rougeot, C., Clarke, P.B., Lepouse, C., Thierry, A.M., Vidal, C., 1999. Nicotinic receptors in the rat prefrontal cortex: increase in glutamate release and facilitation of mediodorsal thalamo-cortical transmission. Eur. J. Neurosci. 11, 18–30.
Gray, R., Rajan, A.S., Radcliffe, K.A., Yakehiro, M., Dani, J.A., 1996. Hippocampal synaptic transmission enhanced by low concentrations of nicotine. Nature 383, 713–716.
Green, M.F., Kern, R.S., Heaton, R.K., 2004. Longitudinal studies of cognition and functional outcome in schizophrenia: implications for MATRICS. Schizophr. Res. 72, 41–51.
Groenewegen, H.J., 1988. Organization of the afferent connections of the mediodorsal thalamic nucleus in the rat, related to the mediodorsal-prefrontal topography. Neuroscience 24, 379–431.
Guldin, W.O., Pritzel, M., Markowitsch, H.J., 1981. Prefrontal cortex of the mouse defined as cortical projection area of the thalamic mediodorsal nucleus. Brain Behav. Evol. 19, 93–107.
Harrison, P.J., 2004. The hippocampus in schizophrenia: a review of the neuropathological evidence and its pathophysiological implications. Psychopharmacol. Berl. 174, 151–162.
Hascup, K.N., Rutherford, E.C., Quintero, J.E., Day, B.K., Nickell, J.R., Pomerleau, F., Huettl, P., Burmeister, J.J., Gerhardt, G.A., 2007. Second-by-second measures of L-glutamate and other neurotransmitters using enzyme-based microelectrode arrays. In: Michael, A.C., Borland, L.M. (Eds.), Electrochemical Methods for Neuroscience, Boca Raton (FL).
Hilti, C.C., Delko, T., Orosz, A.T., Thomann, K., Ludewig, S., Geyer, M.A., Vollenweider, F.X., Feldon, J., Cattapan-Ludewig, K., 2010. Sustained attention and planning deficits but intact attentional set-shifting in neuroleptic-naive first-episode schizophrenia patients. Neuropsychobiology 61, 79–86.
Hinzman, J.M., Thomas, T.C., Burmeister, J.J., Quintero, J.E., Huettl, P., Pomerleau, F., Gerhardt, G.A., Lifshitz, J., 2010. Diffuse brain injury elevates tonic glutamate levels and potassium-evoked glutamate release in discrete brain regions at two days post-injury: an enzyme-based microelectrode array study. J. Neurotrauma 27, 889–899.
Hoover, W.B., Vertes, R.P., 2007. Anatomical analysis of afferent projections to the medial prefrontal cortex in the rat. Brain Struct. Funct. 212, 149–179.
Jay, T.M., Thierry, A.M., Wiklund, L., Glowinski, J., 1992. Excitatory amino acid pathway from the hippocampus to the prefrontal cortex. Contribution of AMPA receptors in hippocampo-prefrontal cortex transmission. Eur. J. Neurosci. 4, 1285–1295.
Jay, T.M., Witter, M.P., 1991. Distribution of hippocampal CA1 and subicular efferents in the prefrontal cortex of the rat studied by means of anterograde transport of Phaseolus vulgaris-leucoagglutinin. J. Comp. Neurol. 313, 574–586.
Konradsson-Geuken, A., Gash, C.R., Alexander, K., Pomerleau, F., Huettl, P., Gerhardt, G.A., Bruno, J.P., 2009. Second-by-Second analysis of alpha 7 nicotine receptor regulation of glutamate release in the prefrontal cortex of awake rats. Synapse 63, 1069–1082.
Lambe, E.K., Picciotto, M.R., Aghajanian, G.K., 2003. Nicotine induces glutamate release from thalamocortical terminals in prefrontal cortex. Neuropsychopharmacology 28, 216–225.
Leonard, C.M., 1969. The prefrontal cortex of the rat. I. Cortical projection of the mediodorsal nucleus. II. Efferent connections. Brain Res. 12, 321–343.
Lewis, D.A., Gonzalez-Burgos, G., 2008. Neuroplasticity of neocortical circuits in schizophrenia. Neuropsychopharmacology 33, 141–165.
Lipska, B.K., Halim, N.D., Segal, P.N., Weinberger, D.R., 2002. Effects of reversible inactivation of the neonatal ventral hippocampus on behavior in the adult rat. J. Neurosci. 22, 2835–2842.
Lipska, B.K., Lerman, D.N., Khaing, Z.Z., Weinberger, D.R., 2003. The neonatal ventral hippocampal lesion model of schizophrenia: effects on dopamine and GABA mRNA markers in the rat midbrain. Eur. J. Neurosci. 18, 3097–3104.
Lipska, B.K., Swerdlow, N.R., Geyer, M.A., Jaskiw, G.E., Braff, D.L., Weinberger, D.R., 1995. Neonatal excitotoxic hippocampal damage in rats causes post-pubertal changes in prepulse inhibition of startle and its disruption by apomorphine. Psychopharmacol. Berl. 122, 35–43.
Lipska, B.K., Weinberger, D.R., 2002. A neurodevelopmental model of schizophrenia: neonatal disconnection of the hippocampus. Neurotox. Res. 4, 469–475.
Luck, S.J., Gold, J.M., 2008. The construct of attention in schizophrenia. Biol. Psychiatry 64, 34–39.
Meyer, F., Peterschmitt, Y., Louilot, A., 2009. Postnatal functional inactivation of the entorhinal cortex or ventral subiculum has different consequences for latent inhibition-related striatal dopaminergic responses in adult rats. Eur. J. Neurosci. 29, 2035–2048.
Meyer, F.F., Louilot, A., 2011. Latent inhibition-related dopaminergic responses in the nucleus accumbens are disrupted following neonatal transient inactivation of the ventral subiculum. Neuropsychopharmacology 36, 1421–1432.
Mitchell, C.P., Grayson, D.R., Goldman, M.B., 2005. Neonatal lesions of the ventral hippocampal formation alter GABA-A receptor subunit mRNA expression in adult rat frontal pole. Biol. Psychiatry 57, 49–55.
Narahashi, T., 1972. Mechanism of action of tetrodotoxin and saxitoxin on excitable membranes. Fed. Proc. 31, 1124–1132.
Neigh, G.N., Arnold, H.M., Rabenstein, R.L., Sarter, M., Bruno, J.P., 2004. Neuronal activity in the nucleus accumbens is necessary for performance-related increases in cortical acetylcholine release. Neuroscience 123, 635–645.
Nuechterlein, K.H., Green, M.F., Kern, R.S., Baade, L.E., Barch, D.M., Cohen, J.D., Essock, S., Fenton, W.S., Frese 3rd, F.J., Gold, J.M., Goldberg, T., Heaton, R.K., Keefe, R.S., Kraemer, H., Mesholam-Gately, R., Seidman, L.J., Stover, E., Weinberger, D.R., Young, A.S., Zalcman, S., Marder, S.R., 2008. The MATRICS consensus cognitive battery, part 1: test selection, reliability, and validity. Am. J. Psychiatry 165, 203–213.
Pantelis, C., Barnes, T.R., Nelson, H.E., Tanner, S., Weatherley, L., Owen, A.M., Robbins, T.W., 1997. Frontal-striatal cognitive deficits in patients with chronic schizophrenia. Brain 120 (Pt 10), 1823–1843.
Paxinos, G., Watson, C., 1998. The Rat Brain I Stereotaxic Coordinates, Fourth ed. Sydney, Australia.
Peterschmitt, Y., Meyer, F., Louilot, A., 2008. Differential influence of the ventral subiculum on dopaminergic responses observed in core and dorsomedial shell subregions of the nucleus accumbens in latent inhibition. Neuroscience 154, 898–910.
Prouteau, A., Verdoux, H., Briand, C., Lesage, A., Lalonde, P., Nicole, L., Reinharz, D., Stip, E., 2005. Cognitive predictors of psychosocial functioning outcome in schizophrenia: a follow-up study of subjects participating in a rehabilitation program. Schizophr. Res. 77, 343–353.
Rutherford, E.C., Pomerleau, F., Huettl, P., Stromberg, I., Gerhardt, G.A., 2007. Chronic second-by-second measures of L-glutamate in the central nervous system of freely moving rats. J. Neurochem. 102, 712–722.
Sarter, M., Lustig, C., Taylor, S.F., 2012. Cholinergic contributions to the cognitive symptoms of schizophrenia and the viability of cholinergic treatments. Neuropharmacology 62, 1544–1553.
Shimamoto, K., Lebrun, B., Yasuda-Kamatani, Y., Sakaitani, M., Shigeri, Y., Yumoto, N., Nakajima, T., 1998. DL-threo-beta-benzyloxyaspartate, a potent blocker of excitatory amino acid transporters. Mol. Pharmacol. 53, 195–201.
St Peters, M., Demeter, E., Lustig, C., Bruno, J.P., Sarter, M., 2011. Enhanced control of attention by stimulating mesolimbic-corticopetal cholinergic circuitry. J. Neurosci. 31, 9760–9771.
Stefani, M.R., Moghaddam, B., 2005. Systemic and prefrontal cortical NMDA receptor blockade differentially affect discrimination learning and set-shift ability in rats. Behav. Neurosci. 119, 420–428.
Sutor, B., Luhmann, H.J., 1995. Development of excitatory and inhibitory postsynaptic potentials in the rat neocortex. Perspect. Dev. Neurobiol. 2, 409–419.
Thoma, P., Wiebel, B., Daum, I., 2007. Response inhibition and cognitive flexibility in schizophrenia with and without comorbid substance use disorder. Schizophr. Res. 92, 168–180.
Tseng, K.Y., Chambers, R.A., Lipska, B.K., 2009. The neonatal ventral hippocampal lesion as a heuristic neurodevelopmental model of schizophrenia. Behav. Brain Res. 204, 295–305.
Tseng, K.Y., Lewis, B.L., Hashimoto, T., Sesack, S.R., Kloc, M., Lewis, D.A., O'Donnell, P., 2008. A neonatal ventral hippocampal lesion causes functional deficits in adult prefrontal cortical interneurons. J. Neurosci. 28, 12691–12699.

Wei, J., Pan, X., Pei, Z., Wang, W., Qiu, W., Shi, Z., Xiao, G., 2012. The beta-lactam antibiotic, ceftriaxone, provides neuroprotective potential via anti-excitotoxicity and anti-inflammation response in a rat model of traumatic brain injury. J. Trauma Acute Care Surg. 73, 654–660.

Westphalen, R.I., Kwak, N.B., Daniels, K., Hemmings Jr., H.C., 2011. Regional differences in the effects of isoflurane on neurotransmitter release. Neuropharmacology 61, 699–706.

Zhang, Y., Guzinski, M., Eger 2nd, E.I., Laster, M.J., Sharma, M., Harris, R.A., Hemmings Jr., H.C., 2010. Bidirectional modulation of isoflurane potency by intrathecal tetrodotoxin and veratridine in rats. Br. J. Pharmacol. 159, 872–878.

Zmarowski, A., Sarter, M., Bruno, J.P., 2007. Glutamate receptors in nucleus accumbens mediate regionally selective increases in cortical acetylcholine release. Synapse 61, 115–123.